# Energy-Aware Ergodic Search: Continuous Long-Term Exploration for Multiagent Systems

Adam Seewald[1], Marvin Chancán[1], Cameron J. Lerch[1], Hector Castillo[1], Aaron M. Dollar[1], and Ian Abraham[1]

*Abstract——*

*Index Terms*—Motion and Path Planning; Energy and Environment-Aware Autonomation.

## I. INTRODUCTION

**A** A

## II. PROBLEM FORMULATION

This work addresses the problem of exploring a bounded space with multiple agents, continuously, and proportionally to a spatial distribution. In the remainder of the text, we will use the term "continuously" to indicate that there is at least one agent that is exploring the space at all times.

Canonical ergodic search [1–7] does not deal with continuous exploration. It derives an agent's control – or analogously multiple agents control [8–12] – so that its trajectory maximizes an ergodic metric defined in the spectral domain [13].

**Problem II.1** (Ergodic search). Consider a bounded space $\mathcal{Q} \subset \mathbb{R}^D$ of dimension $D$ with $D \in \mathbb{N}_{>0}$ and a spatial distribution $\phi$. *Ergodic search problem* is the problem of deriving a control action $\mathbf{u}(t) \in \mathcal{U} \subset \mathbb{R}^V$ with $V \in \mathbb{N}_{>0}$ so that the trajectory $\mathbf{q}(t) \in \mathcal{Q}$ is proportional to the spatial distribution $\phi$.

Here the notation $\mathbb{R}$ and $\mathbb{N}$ indicates reals and naturals, $\mathbb{N}_{>0}$ strictly naturals. Bold notation is used for vectors.

We extend the canonical ergodic search problem to multi-agent continuous ergodic search, i.e., exploration with multiple agents under spatial distribution and battery constraints.

**Problem II.2** (Multi-agent continuous ergodic search). Consider a set of $n$ agents $\boldsymbol{\alpha} := \{\alpha_1, \alpha_2, \ldots, \alpha_n\}$, a bounded space $\mathcal{Q}$, and a spatial distribution $\phi$ similar to Problem II.1. *Multi-agent continuous ergodic search problem* is the problem of deriving each agent $^j\alpha$ control action $^j\mathbf{u}(t)$ so that its trajectory $^j\mathbf{q}(t)$ is proportional to the spatial distribution $\phi$ on a continuous time horizon.

We will provide a solution to Problem II.2 (see Section III), assuming that there are one or more areas in $\mathcal{Q}$ – namely, charging stations – where the agents $\boldsymbol{\alpha}$ can land and recharge the battery, e.g., using wireless charging (see Sec. IV).

[1]A. S., M. C., C. J. L., H. C., A. M. D., and I. A. are with the Department of Mechanical Engineering and Materials Science, Yale University, CT, USA. Email: adam.seewald@yale.edu;

## III. METHODS

In this section, we discuss the methods utilized in this work for continuous exploration with multiple agents and proportionally to a spatial distribution

We discuss how to achieve the latter in Sec. III-A and the former in Sec. III-B.

### A. Ergodic search

To derive an agent's trajectory proportionally to a spatial distribution, canonical ergodic search first requires defining the distribution $\phi$.

For the purposes of this, in both Problem II.1 and II.2, let us consider a Gaussian mixture model (GMM)

$$\phi(\boldsymbol{\delta}, \mathbf{q}) := \sum_{k=1}^{m} \delta_k \mathcal{N}(\mathbf{q} \,|\, \mu_k, \Sigma_k), \tag{1}$$

composed of $m$ Gaussians. Each has a covariance matrix $\Sigma_k \in \mathbb{R}^{D \times D}$, a center $\mu_k \in \mathcal{Q}$, and a positive mixing coefficient $\delta_k \in \boldsymbol{\delta}$ such that the sum of the $\delta$s is less or equal to one. They indicate how well is each Gaussian in the GMM considered.

The goal of the ergodic search is to minimize an ergodic metric [1]

$$\mathcal{E}(\boldsymbol{\delta}, \mathbf{q}(t)) := \frac{1}{2} \sum_{k \in \mathcal{K}} \Lambda_k \big( c_k(\mathbf{q}(t)) - \phi_k(\boldsymbol{\delta}) \big)^2, \tag{2}$$

where $\phi_k$ are coefficients derived utilizing the Fourier series on the spatial distribution $\phi$ and $c_k$ on the trajectory $\mathbf{q}(t)$. They are detailed in Equation (6) and (4) respectively. $\Lambda_k$ is a weight factor. That is, if

$$\Lambda_k = (1 + \|k\|^2)^{(-D-1)/2}, \tag{3}$$

lower frequencies have more weight [4]. $\mathcal{K} \in \mathbb{N}^D$ is a set of index vectors that covers $[K] \times \cdots \times [K] \in \mathbb{N}^{K^D}$ where $K$ is a given number of frequencies including the fundamental frequency [13]. The notation $[K]$ indicates positive naturals up to $K$.

The coefficients $c_k$ are derived using the Fourier series basis function. If we consider the trigonometric form, they can be expressed

$$c_k(\mathbf{q}(t)) := \int_{\mathcal{T}} \frac{1}{L^D} \prod_{d \in [D]_{>0}} \big( \cos(k_d \, \mathbf{q}_d(\tau) \, \psi) - i \sin(k_d \, \mathbf{q}_d(\tau) \, \psi) \big) \, d\tau / t, \tag{4}$$

where $\psi$ is $2\pi/L$ for a given period $L \in \mathbb{R}_{>0}$, $i$ is the imaginary unit, $k_d$ is the $d$th item of $k$, and $\mathbf{q}_d$ the $d$th item of $\mathbf{q}$.

$\mathcal{T}$ is built so that the integration is between $\tau = t_0$ and $t$, and the notation $[D]_{>0}$ indicates strictly positive naturals up to $D$.

$c_k$ is evaluated per each $k$ in $\mathcal{K}$ in Eq. (2).

To derive the coefficients $\phi_k$, let us consider the GMM model in Eq. (1) on a search space $\mathcal{Q}$. The space is further bounded to a symmetric set $[-L/2, L/2]^D$ since the Gaussians are symmetric about the zero axes. The resulting new model is then

$$\Phi(\boldsymbol{\delta}, \mathbf{q}) := \sum_{d \in [2^D]_{>0}} \sum_{k=1}^{m} \delta_k \, \mathcal{N}(\mathbf{q} \,|\, A_d \mu_k, A_d \Sigma_k A_d^T)/2^D, \quad (5)$$

where $A_d \in \mathbb{R}^{D \times D}$ are linear transformation matrices [13]. Let us call the integrand in Eq. (4) $c : \mathcal{Q} \longrightarrow \mathbb{R}^K$. It maps the space to the spectral domain. The equivalent of Eq. (4) for the spatial distribution can be then expressed

$$\phi_k(\boldsymbol{\delta}) := \int_{\mathcal{Q}} \Phi(\boldsymbol{\delta}, \mathbf{q}) \, c(\mathbf{q}) \, d\mathbf{q}. \quad (6)$$

$\mathcal{Q}$ is built so that the integration is within the points of the bounded symmetric set $\mathbf{q} \in [-L/2, L/2]^D$.

$\phi_k$ is evaluated per each $k$ in $\mathcal{K}$ in Eq. (2).

Let us first formulate the solution for Problem II.1, borrowed by canonical ergodic search. If the agent's dynamics is described by a generic differential equation $\dot{\mathbf{q}}(t) = f(\mathbf{q}(t), \mathbf{u}(t))$, an optimal control problem (OCP) that selects an ergodic control action can be formulated as [14]

$$\min_{\mathbf{q}(t), \mathbf{u}(t)} \int_{\mathcal{T}} \mathbf{u}(\tau)^T R \mathbf{u}(\tau) \, d\tau + \mathcal{E}(\boldsymbol{\delta}, \mathbf{q}(t)), \quad (7a)$$

$$\text{s.t. } \dot{\mathbf{q}} = f(\mathbf{q}(t), \mathbf{u}(t)), \quad (7b)$$

$$\mathbf{q}(t) \in \mathcal{Q}, \, \mathbf{u}(t) \in \mathcal{U}, \quad (7c)$$

$$\mathbf{q}(t_0), \mathbf{q}(t_f) \text{ are given}, \quad (7d)$$

where the ergodic metric is derived in Eq. (2), $R \in \mathbb{R}^{V \times V}$ is a control penalizing diagonal positive-definite matrix, and $t_0, t_f$ are respectively the first and last time instants. $\mathcal{T}$ is $[t_0, t_f)$.

To formulate the solution to Problem II.2, let us first extend the OCP in Eq. (7) to multiagent systems [9]. Eq. (7a) becomes
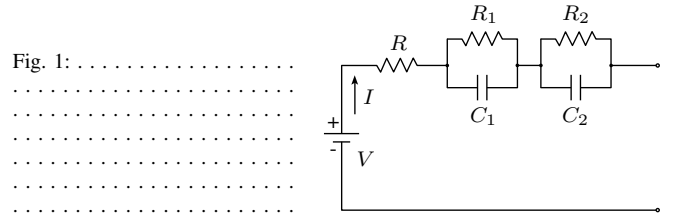
$$\min_{\square} \sum_{k=1}^{n} \left( \int_{\mathcal{T}_k} {}^k\mathbf{u}(\tau)^T R_k \, {}^k\mathbf{u}(\tau) \, d\tau + \mathcal{E}(\boldsymbol{\delta}, {}^k\mathbf{q}(t)) \right), \quad (8)$$

where the ergodic metric and the control penalizing term $R_k$ are now agent-specific. The term $\square$ is ${}^1\mathbf{q}(t), {}^2\mathbf{q}(t), \ldots, {}^n\mathbf{q}(t), {}^1\mathbf{u}(t), {}^2\mathbf{u}(t), \ldots {}^n\mathbf{u}(t)$. $\mathcal{T}_k$ is $[{}^kt_0, {}^kt_f)$, i.e., different agents might have different duration.

Let us consider a vector $\mathbf{b} \in \mathbb{R}^3$ – which is detailed later in Sec. III-B – whose trajectory $\mathbf{b}(t)$ describes the battery metrics' evolution in time. If $\mathbf{b}_{\text{SoC}}$ is the value of the vector that expresses the battery state of charge (SoC), the expression in Eq. (8) might select ergodic metrics corresponding to trajectories that are impossible to traverse in the $\mathbf{b}_{\text{SoC}} \in (0, 1]$ domain, i.e., one or more agents' state at $\mathbf{q}(t_f)$ will not satisfy Eq. (7d).

In order to satisfy the battery SoC domain and always keep at least one agent exploring, an OCP must satisfy an additional constrain

$$\exists k \in [n] \text{ s.t. } {}^k\mathbf{b}_{\text{SoC}}(t_f) \in (0, b_f], \quad (9)$$



Fig. 1: . . . . . . . . . . . . . . . . .
. . . . . . . . . . . . . . . . . . . . .
. . . . . . . . . . . . . . . . . . . . .
. . . . . . . . . . . . . . . . . . . . .
. . . . . . . . . . . . . . . . . . . . .
. . . . . . . . . . . . . . . . . . . . .
. . . . . . . . . . . . . . . . . . . . .

where $b_f \in (0, 1) \subset \mathbb{R}_{>0}$ is a given desired battery SoC at the final time instant.

Finally, let us consider the realistic assumption that the optimization horizon $N \in \mathbb{R}_{>0}$ is known and is, e.g., an empirically collected value that corresponds to one of the agents' discharge times (see Sec. IV).

The OCP that provides a solution to Problem II.2 can be formulated as

$$\min_{\square, \boldsymbol{\delta}} \sum_{k=1}^{n} \int_{\mathcal{T}_k} {}^k\mathbf{u}(\tau)^T R_k \, {}^k\mathbf{u}(\tau) \, d\tau - \sum_{k=1}^{m} \delta_k, \quad (10a)$$

$$\text{s.t. } {}^1\dot{\mathbf{q}}(t) = f_1({}^1\mathbf{q}(t), {}^1\mathbf{u}(t)), \ldots, {}^n\dot{\mathbf{q}}(t) = f_n({}^n\mathbf{q}(t), {}^n\mathbf{u}(t)), \quad (10b)$$

$${}^1\mathbf{q}(t), \ldots, {}^n\mathbf{q}(t) \in \mathcal{Q}, \, {}^1\mathbf{u}(t), \ldots, {}^n\mathbf{u}(t) \in \mathcal{U}, \quad (10c)$$

$$\exists k \in [n] \text{ s.t. } {}^k\mathbf{b}_{\text{SoC}}(t_f) \in (0, b_f], \quad (10d)$$

$$\forall k \, \mathcal{E}(\boldsymbol{\delta}, {}^k\mathbf{q}(t)) \leq \gamma, \quad (10e)$$

$$g_1(\boldsymbol{\delta}, {}^1\mathbf{q}(t), {}^1\mathbf{u}(t)) \leq 0, \ldots, g_n(\boldsymbol{\delta}, {}^n\mathbf{q}(t), {}^n\mathbf{u}(t)) \leq 0, \quad (10f)$$

$${}^1\mathbf{q}(t_0), {}^1\mathbf{q}(t_f), \ldots, {}^n\mathbf{q}(t_0), {}^n\mathbf{q}(t_f), b_f, \gamma \text{ are given}, \quad (10g)$$

where constraints in Eq. (10f) are optional and express additional requirements, e.g., that there is always at least one agent exploring $\mathcal{Q}$, the agents explore the space two-by-two, etc. (see Sec. IV).

In Eq. (10), the ergodic metric is integrated into the constraint as proposed in [15]. The cost contains further mixing coefficient $\boldsymbol{\delta}$ in Eq. (1) – so that one can find tradeoffs between the single Gaussians, the different agents, and the battery SoC (see Sec IV).

### B. Battery modeling

To derive a battery model for continuous exploration – a model that allows us to predict when an agent is exploring and when it conversely should be recharging the battery – let us consider an equivalent circuit model (ECM). These models are commonly employed in battery metrics estimation for robots and other applications, especially if equipped with rechargeable battery cells [16–21].

The ECM model we employ is a second-order RC model [22], as illustrated in Figure 1 [23].

Formally, it can be formulated as [22]

$$\dot{\mathbf{b}}(t) = \begin{bmatrix} -1/(R_1 C_1) & 0 & 0 \\ 0 & -1/(R_2 C_2) & 0 \\ 0 & 0 & 0 \end{bmatrix} \mathbf{b}(t) - \begin{bmatrix} -1/C_1 \\ -1/C_2 \\ \zeta/Q \end{bmatrix} I(t), \quad (11)$$

where $\zeta \in \mathbb{R}$ is a battery coefficient [21], $R_1, R_2 \in \mathbb{R}$ and $C_1, C_2 \in \mathbb{R}$ are the resistors and capacitors relative to the first and second RC elements in the ECM measured in ohms and farad respectively. $Q \in \mathbb{R}$ is the battery nominal capacity measured in amperes per hour.
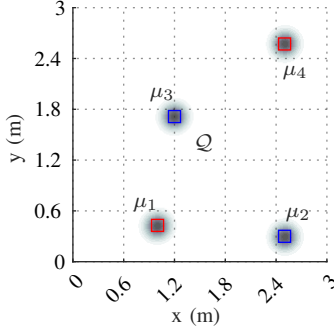
Fig. 2: . . . . . . . . . . . . . . . . . . . . . .

$I \in \mathbb{R}$ is then the internal current which is load-dependent, e.g., the current required to run the motors, actuators, etc.

The state $\mathbf{b} := \begin{bmatrix} V_1 & V_2 & \mathbf{b}_{\text{SoC}} \end{bmatrix} \in \mathbb{R}^3$ contains three battery metrics. $V_1, V_2 \in \mathbb{R}$ are the voltages measured in volts across the first and second RC elements, and $\mathbf{b}_{\text{SoC}} \in (0,1]$ is the normalized battery SoC that evolves from fully charged – or from a given initial value $\mathbf{b}_{\text{SoC}}(t_0)$ – to discharged.

The battery voltage at the extremes of the ECM $V_e \in \mathbb{R}$, measured in volts, can be then formulated as [22]

$$V_e(t) = V_{\text{OC}}(\mathbf{b}_{\text{SoC}}(t)) - V_1(t) - V_2(t) - I(t)R, \quad (12)$$

where $R \in \mathbb{R}$ is the single resistor measured in ohm in Fig. 1, and $V_{\text{OC}}$ is the open circuit voltage. It is a nonlinear function of the battery SoC and can be retrieved from the battery data sheet [19].

The values of $R_1, C_1, R_2, C_2, R$ are identified so that the model output and the physical behavior of the agents are matched as closely as possible [22] (see Sec. IV).

The battery model allows us to determine the battery SoC $\mathbf{b}_{\text{SoC}}$ in Eq. (10d), which is in turn utilized to find the control action $\mathbf{u}(t)$ so that there is at least one agent exploring $\mathcal{Q}$ at all times. This means that when the solution of the OCP in Eq. (10) is evaluated, the battery model in Eq. (11) is integrated for the duration of the horizon, whereas the recharging is approximated linear $\mathbf{b}_{\text{SoC}} = \eta\,\mathbf{b}_{\text{SoC}} + \theta$ for a given $\eta, \theta \in \mathbb{R}$.

## IV. EXPERIMENTAL RESULTS

In this section, we discuss our experimental setup and results. Our experiments are implemented first in simulation using MATLAB (R), and physical experiments are implemented in Python and conducted using a set of Crazyflie 2.0 micro aerial vehicles (MAVs).

In both cases, the source code[1] is released under the popular non-commercial open-source license CC BY NC-SA 4.0. The solution of the OCP in Eq. (10) relies on two external open-source components from the literature: the popular nonlinear programming solver IPOPT [24] and a software framework for nonlinear optimization called CasADi [25].

We evaluate our approach under two different scenarios. In both the scenarios, we derive a continuous ergodic exploration of a three-by-three-meter space $\mathcal{Q}$. The spatial distribution $\phi$ contains four Gaussians in the GMM in Eq. (1), as illustrated in Fig. 2.

In the first extensive scenario, four MAVs $\alpha_1, \alpha_2, \alpha_3$, and $\alpha_4$ are placed on top of four wireless charging stations. Each

MAV is equipped with a positioning and wireless charging decks. Precise positioning of MAVs is achieved via two HTC SteamVR Base Station 2.0 units. Each MAV is then equipped with a one-cell 250 mAh 3.7 volts LiPo battery, capable of approximately seven minutes of flight. The optional constraints in Eq. (10f) are built so that each MAV covers two Gaussians at a time that are respectively farthest (see different colors in Fig. 2), whereas the battery constraint is edited so that there are two MAVs at each time, i.e.,

$$\exists_{=1} k_1, k_2 \in [n] \text{ s.t. } {}^{k_1}\mathbf{b}_{\text{SoC}}, {}^{k_2}\mathbf{b}_{\text{SoC}} \in (0, b_f), \quad (13)$$

where the notation $\exists_{=1}$ indicates the unique existential quantification. The horizon is derived empirically and is set to two minutes and a half. The battery values used in the scenario are those proposed in [22], whereas the battery and recharging coefficients are derived empirically [21]. The ergodicity metric in Eq. (2) is set to be lower or equal to 0.05 via the constraint in Eq. (10e), in line with similar literature [15].

The results are shown in Fig. 3. The figure is to be read from left to right and from top to bottom, with the horizon being indicated under each subfigure (meaning that $t_0$ is the first horizon, $t_1$ is the second horizon, etc.). Initially, two MAVs are selected via the solution to the OCP in Eq. (10), $\alpha_1$ and $\alpha_2$. They are located at coordinates $(0.3, 0.9)$ and $(2.7, 2.1)$ respectively, denoted by the blue and red filled squares. The energy-aware ergodic trajectories ${}^1\mathbf{q}(t)$ and ${}^2\mathbf{q}(t)$ are selected so that the MAVs land at each other's charging stations, i.e., ${}^1\mathbf{q}(t_f) = {}^2\mathbf{q}(t_0)$ and vice-versa. The mixing coefficients for $\alpha_1$ are such that $\delta_2 > \delta_3$, meaning that the agent $\alpha_1$ explores in more detail the area delimited by the Gaussian centered in $\mu_2$. This is indicated by the darker coloring of the different Gaussians, which is proportional to the optimal value of $\boldsymbol{\delta}$.

An analogous situation is to be observed with agent $\alpha_2$. At the end of the optimization horizon, both agents land in the proximity of each other's charging stations (the red and blue filled dots at the end of the trajectories for respectively $\alpha_2$ and $\alpha_1$), meaning that the constraint in Eq. (10g) is evaluated within

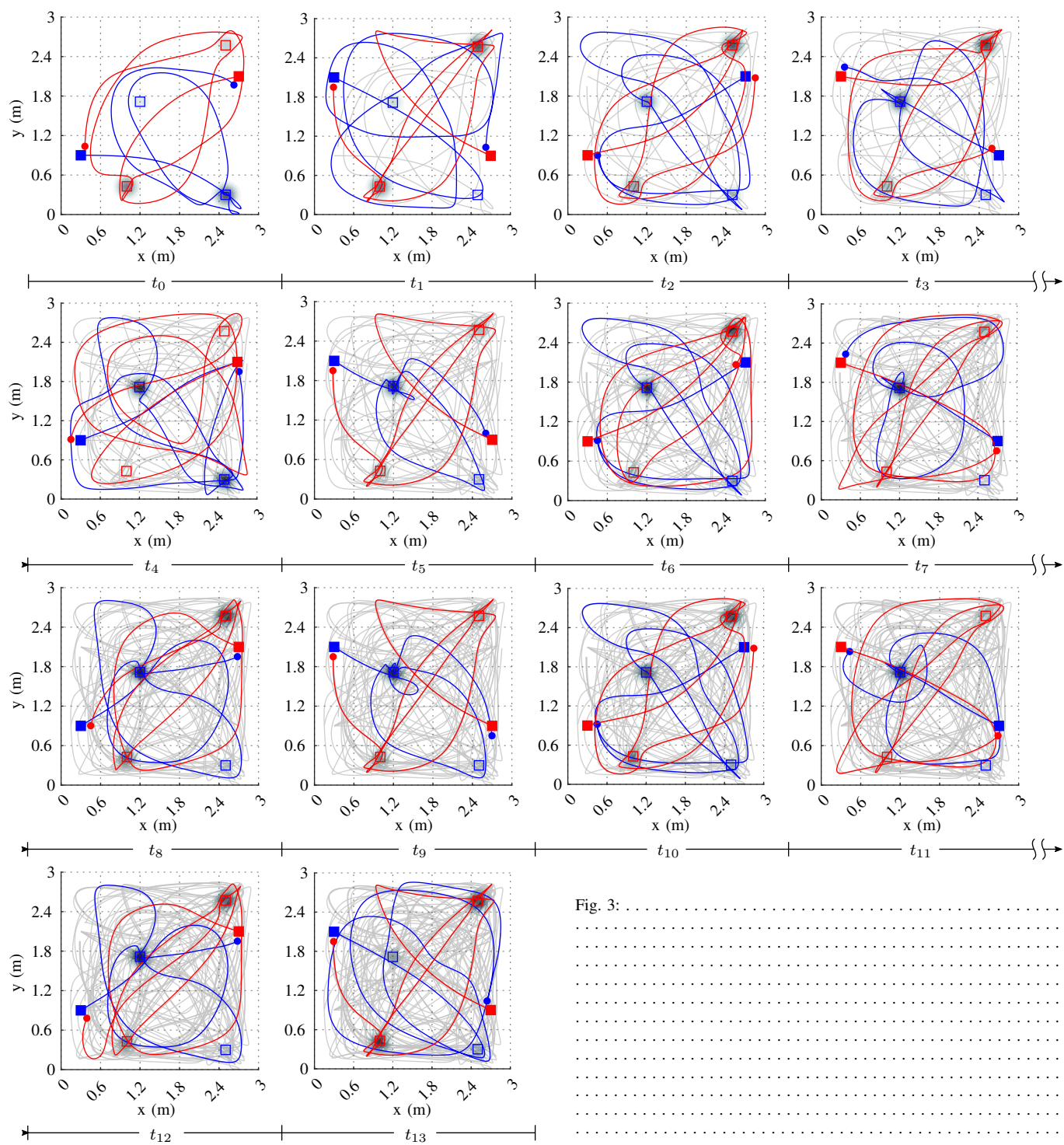$$\|{}^{k_2}\mathbf{q}(t_f) - {}^{k_1}\mathbf{q}(t_0)\| \le \varepsilon, \quad (14)$$

where $\varepsilon \in \mathbb{R}_{>0}$ and $k_1, k_2 \in [n]$ are given.

Once the two agents $\alpha_1$ and $\alpha_2$ land, they start recharging. The formulation of the OCP in Eq. (10) is such that the other two agents $\alpha_3$ and $\alpha_4$ are selected. They are located at coordinates $(0.3, 2.1)$ and $(2.7, 0.9)$ respectively. They proceed on the respective energy-aware ergodic trajectories and land at each other's charging stations, with the past trajectory being indicated in the background in gray. The figure shows fourteen horizons. The actual exploration in the scenario, however, is continuous.

## V. CONCLUSION AND FUTURE DIRECTIONS

—

Fig. 3: . . . . . . . . . . . . . . . . . . . . . . . . . . . . . . . . . . . . . . . . . . . . . . . . . . . . . . . . . . . . . . . . . . . . . . . . . . . . . . . . . . . . . . . . . . . . . . . . . . . . . . . . . . . . . . . . . . . . . . . . . . . . . . . . . . . . . . . . . . . . . . . . . . . . . . . . . . . . . . . . . . . . . . . . . . . . . . . . . . . . . . . . . . . . . . . . . . . . . . . . . . . . . . . . . . . . . . . . . . . . . . . . . . . . . . . . . . . . . . . . . . . . . . . . . . . . . . . . . . . . . . . . . . . . . . . . . . . . . . . . . . . . . . . . . . . . . . . . . . . . . . . . . . . . . . . . . . . . . . . . . . . . . . . . . . . . . . . . . . . . . . . . . . . . . . . . . . . . . . . .

## REFERENCES

[1] G. Mathew and I. Mezić, "Metrics for ergodicity and design of ergodic dynamics for multi-agent systems," *Physica D: Nonlinear Phenomena*, vol. 240, no. 4, pp. 432–442, 2011. 1

[2] L. M. Miller and T. D. Murphey, "Trajectory optimization for continuous ergodic exploration," in *IEEE American Control Conference*, 2013, pp. 4196–4201. 1

[3] I. Abraham, A. Prabhakar, and T. D. Murphey, "An ergodic measure for active learning from equilibrium," *IEEE Transactions on Automation Science and Engineering*, vol. 18, no. 3, pp. 917–931, 2021. 1

[4] L. M. Miller, Y. Silverman, M. A. MacIver, and T. D. Murphey, "Ergodic exploration of distributed information," *IEEE Transactions on Robotics*, vol. 32, no. 1, pp. 36–52, 2016. 1

[5] L. Dressel and M. J. Kochenderfer, "On the optimality of ergodic trajectories for information gathering tasks," in *IEEE American Control Conference*, 2018, pp. 1855–1861. 1

[6] G. De La Torre, K. Flaßkamp, A. Prabhakar, and T. D. Murphey, "Ergodic exploration with stochastic sensor dynamics," in *IEEE American Control Conference*, 2016, pp. 2971–2976. 1

[7] S. Shetty, J. Silvério, and S. Calinon, "Ergodic exploration using tensor train: Applications in insertion tasks," *IEEE Transactions on Robotics*, vol. 38, no. 2, pp. 906–921, 2022. 1

[8] A. Prabhakar, I. Abraham, A. Taylor, M. Schlafly, K. Popovic, G. Diniz, B. Teich, B. Simidchieva, S. Clark, and T. Murphey, "Ergodic specifications for flexible swarm control: From user commands to persistent adaptation," in *Robotics: Science and Systems*, 2020, p. 9. 1

[9] H. Coffin, I. Abraham, G. Sartoretti, T. Dillstrom, and H. Choset, "Multi-agent dynamic ergodic search with low-information sensors," in *IEEE International Conference on Robotics and Automation*, 2022, pp. 11 480–11 486. 1, 2

[10] C. Lerch, D. Dong, and I. Abraham, "Safety-critical ergodic exploration in cluttered environments via control barrier functions," in *IEEE International Conference on Robotics and Automation*, 2023, pp. 10 205–10 211. 1

[11] I. Abraham and T. D. Murphey, "Decentralized ergodic control: Distribution-driven sensing and exploration for multiagent systems," *IEEE Robotics and Automation Letters*, vol. 3, no. 4, pp. 2987–2994, 2018. 1

[12] S. Patel, S. Hariharan, P. Dhulipala, M. C. Lin, D. Manocha, H. Xu, and M. Otte, "Multi-agent ergodic coverage in urban environments," in *IEEE International Conference on Robotics and Automation*, 2021, pp. 8764–8771. 1

[13] S. Calinon, *Mixture models for the analysis, edition, and synthesis of continuous time series*. Springer, 2020, pp. 39–57. 1, 2

[14] E. Ayvali, H. Salman, and H. Choset, "Ergodic coverage in constrained environments using stochastic trajectory optimization," in *IEEE/RSJ International Conference on Intelligent Robots and Systems*, 2017, pp. 5204–5210. 2

[15] D. Dong, H. Berger, and I. Abraham, "Time optimal ergodic search," in *Robotics: Science and Systems*, 2023, p. 13. 2, 3

[16] C. Zhang, W. Allafi, Q. Dinh, P. Ascencio, and J. Marco, "Online estimation of battery equivalent circuit model parameters and state of charge using decoupled least squares technique," *Energy*, vol. 142, pp. 678–688, 2018. 2

[17] X. Hu, S. Li, and H. Peng, "A comparative study of equivalent circuit models for li-ion batteries," *Journal of Power Sources*, vol. 198, pp. 359–367, 2012. 2

[18] A. Hasan, M. Skriver, and T. A. Johansen, "eXogenous Kalman filter for state-of-charge estimation in lithium-ion batteries," in *IEEE Conference on Control Technology and Applications*, 2018, pp. 1403–1408. 2

[19] H. Hinz, "Comparison of lithium-ion battery models for simulating storage systems in distributed power generation," *Inventions*, vol. 4, 2019. 2, 3

[20] S. Mousavi G. and M. Nikdel, "Various battery models for various simulation studies and applications," *Renewable and Sustainable Energy Reviews*, vol. 32, pp. 477–485, 2014. 2

[21] A. Seewald, H. García de Marina, H. S. Midtiby, and U. P. Schultz, "Energy-aware planning-scheduling for autonomous aerial robots," in *IEEE/RSJ International Conference on Intelligent Robots and Systems*, 2022, pp. 2946–2953. 2, 3

[22] S. Zhao, S. R. Duncan, and D. A. Howey, "Observability analysis and state estimation of lithium-ion batteries in the presence of sensor biases," *IEEE Transactions on Control Systems Technology*, vol. 25, no. 1, pp. 326–333, 2017. 2, 3

[23] A. Seewald, "Energy-aware coverage planning and scheduling for autonomous aerial robots," Ph.D. dissertation, Syddansk Universitet. Det Tekniske Fakultet, 2021, doi.org/10.21996/7ka6-r457. 2

[24] A. Wächter and L. T. Biegler, "On the implementation of an interior-point filter line-search algorithm for large-scale nonlinear programming," *Mathematical Programming*, vol. 106, no. 1, pp. 25–57, 2006. 3

[25] J. Andersson, J. Åkesson, and M. Diehl, "CasADi: A symbolic package for automatic differentiation and optimal control," in *Recent Advances in Algorithmic Differentiation*. Springer, 2012, pp. 297–307. 3